Journal of Nano- and Electronic Physics
Vol. **13** No 6, 06003(5pp) (2021)

Журнал нано- та електронної фізики
Том **13** № 6, 06003(5cc) (2021)

Enhanced Humidity Sensing Properties of Surfactant-Free Hydrothermally Synthesized Tin Oxide Nanoparticles

T. Preethi[1], K. Senthil[1,*], S. Ashokan[1], R. Balakrishnaraja[2], B. Sundaravel[3], P. Saravanan[4]

[1] *Advanced Materials Research Laboratory, Department of Physics, Bannari Amman Institute of Technology, Sathyamangalam 638401, Tamil Nadu, India*
[2] *Department of Food Technology, Bannari Amman Institute of Technology, Sathyamangalam 638401, Tamil Nadu, India*
[3] *Materials Science Group, Indira Gandhi Centre for Atomic Research, HBNI, Kalpakkam 603102, Tamil Nadu, India*
[4] *Defense Metallurgical Research Laboratory (DMRL), Kanchanbagh, Hyderabad 500058, India*

(Received 01 May 2021; revised manuscript received 03 December 2021; published online 20 December 2021)

Metal oxide semiconductor nanomaterials have been widely used for applications in solar cells, batteries, gas sensors, optoelectronics, photocatalysis and hydrogen generation. Humidity sensors based on metal oxide semiconductors have shown significant contribution in the field of environmental monitoring, food technology and biotechnology. Among the various metal oxide semiconductors, tin oxide (SnO_2) nanoparticles have generated more interest due to their excellent chemical stability, high transparency and low electrical sheet resistance. In the present work, SnO_2 nanoparticles were synthesized by employing a simple hydrothermal process without using any surfactant. The synthesized nanoparticles were investigated using XRD, SEM, EDAX, UV-visible and humidity sensing measurements. The structural property of the sample investigated using XRD analysis indicated that the synthesized SnO_2 nanoparticles have pure crystalline phase with a tetragonal crystal structure of the P42/mnm space group. The surface morphology analyzed using SEM micrograph showed agglomerated nanoparticles without any specific structure. Optical characterization using UV-visible spectroscopy indicated that the synthesized nanoparticles have strong absorption in the UV region. The humidity sensing property analyzed from the variation of electrical resistivity with relative humidity (% RH) showed good hysteresis behavior and the observed variation in electrical conduction is explained based on protonic conduction mechanism on the surface.

Keywords: Metal oxides, SnO_2 nanoparticles, Hydrothermal method, Optical properties, Humidity sensor.

DOI: 10.21272/jnep.13(6).06003 PACS numbers: 73.61.Jc, 71.20.Mq, 88.40.hj, 88.40.jj

1. INTRODUCTION

Semiconductor metal oxide nanomaterials are attracting attention in the field of materials science because of their unique physical and chemical properties at the nanoscale, which are commonly utilized in fundamental research and industrial applications. Advances in research related to metal oxide nanomaterials are phenomenal due to their potential applications in the area of optoelectronics, gas sensors, solar cells, batteries, catalysis and medicine [1]. Among the various metal oxide semiconductors, tin oxide (SnO_2) is considered as a promising semiconductor having a tetragonal rutile structure with a wide band gap for technological applications [2]. In the area of gas sensing technology, metal oxide based sensors have become a hotspot. Water vapor in the air is a critical parameter that has a direct effect on the efficiency of gas sensors. Hence, humidity sensors are important because they provide an accurate estimate of the water vapor content in the atmosphere and these sensors find applications in food technology, crop management, textile industry, anti-corrosion of devices, optoelectronic industrial production, environmental and biomedical processing [3]. Yang et al. [4] synthesized SnO_2 nanoparticles without any template or surfactant at low temperature using a facile solvothermal method and investigated the potential of SnO_2 nanoparticles as an efficient sensor for detecting formaldehyde. By annealing SnSe nanosheets in an argon atmosphere, Zhong et al. [5] developed a humidity sensor based on SnO_2 nanosheets with abundant oxygen vacancies. Tomer and Duhan [6] reported mesoporous SnO_2 and Ag-doped SnO_2 nanostructures synthesized by nanocasting using mesoporous silica (SBA-15) as a hard template for humidity sensor applications. Radovic et al. [7] synthesized SnO_2 nanosheets with multifunctional properties using a hydrothermal method for flexible gas sensors and ultraviolet A (UVA) light sensors. In the present work, SnO_2 nanoparticles are synthesized by hydrothermal method without using any surfactant. The SnO_2 nanoparticles are characterized by analyzing their structural, morphological, optical and humidity sensing properties. The hysteresis behavior and sensitivity of the fabricated SnO_2-based humidity sensor is studied, and the results are compared with the previously reported SnO_2-based humidity sensors.

2. EXPERIMENTAL PROCEDURE

2.1 Synthesis of SnO_2 Nanoparticles

Tin (IV) chloride pentahydrate ($SnCl_4.5H_2O$), sodium hydroxide (NaOH) and methanol (CH_3OH) are the chemicals used for the synthesis of SnO_2 nanoparticles. All the chemicals are used without any further purification. In a typical synthesis, $SnCl_4.5H_2O$ is dissolved in 50 ml of double-deionized water at a molar concen-

* ksenthiludt@gmail.com

tration of 0.4 M. NaOH is added into the prepared solution for adjusting the pH value close to 10. A milky white solution is obtained, and the contents are stirred for 30 min at room temperature (RT). The mixture is then placed in a stainless-steel autoclave lined with Teflon and subjected to a hydrothermal process at 150 °C for 24 h. After completion of the reaction, the autoclave is allowed to cool down automatically. The unreacted impurities are removed by centrifugation and several washes with distilled water and methanol. The final products are dried at 80 °C for 12 h and then calcined at 600 °C for 3 h.

2.2 Characterization Techniques

The phase and structural characterization of the synthesized sample is investigated using Inel Equinox 2000 diffractometer. The surface morphology and composition analysis are evaluated using a scanning electron microscope (SEM, Leo 440i). A UV-visible spectrophotometer (Shimadzu UV-1800) with Xenon lamp as a light source is utilized for optical absorption analysis. A laboratory made set up is employed to investigate humidity sensing properties of the nanoparticles by measuring the variation of electrical resistivity with relative humidity using a LCR meter.

3. RESULTS AND DISCUSSION

3.1 Structural Analysis

The X-ray diffraction pattern of SnO_2 nanoparticles synthesized at 0.4 M is shown in Fig. 1. The diffraction peaks at various diffraction angles are compared with the standard JCPDS data # 41-1445 and the corresponding crystalline planes are indexed. The observed XRD pattern confirms the formation of pure SnO_2 polycrystalline phase, corresponding to a tetragonal crystal system with P42/mnm space group, and is found to be consistent with the previously reported results [4]. The average crystalline size of the SnO_2 nanoparticles evaluated using Debye-Scherrer's formula is found to be 9.4 nm. A dislocation density of 0.01199 lines/m^2 and a microstrain value of 0.2254 indicate the high crystalline nature of the synthesized nanoparticles.

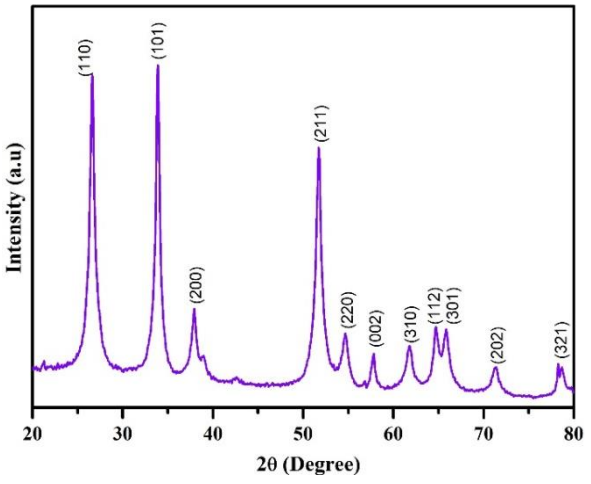

Fig. 1 – XRD pattern of SnO_2 nanoparticles

3.2 Surface Morphology and Composition

The surface morphology and chemical composition of the nanoparticles analyzed using SEM and energy-dispersive spectroscopy (EDS) analysis, respectively, are shown in Fig. 2. The SEM micrograph (Fig. 2a) clearly indicates that the nanoparticles agglomerate without showing any specific structure. Agglomeration of irregularly shaped particles may be due to surface tension and interactive forces [8]. The EDS spectrum (Fig. 2b) confirms the existence of Sn and O as major trace elements. The inset table in the EDS spectrum shows the estimated weight % of trace elements. The peak from Na in both spectra may be due to the use of sodium hydroxide as a precipitating agent.

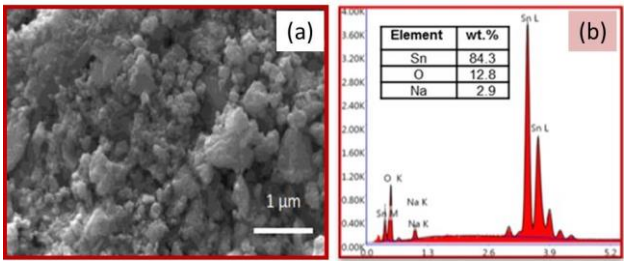

Fig. 2 – (a) SEM micrograph and (b) EDS spectrum of SnO_2 nanoparticles

3.3 Optical Characterization

The UV-visible absorption spectrum recorded in the range of 250-500 nm is shown in Fig. 3. The spectrum shows an absorption peak centered at 334 nm, and the observed peak in the UV region can be associated with the near band edge emission of SnO_2. The band gap energy of the synthesized SnO_2 sample is calculated from the Tauc's plot (inset of Fig. 3) plotted against $(ahv)^2$ on the y-axis and energy (hv) on the x-axis. The band gap energy value is obtained from the intercept of the linear absorption edge part with the energy axis, and the value is found to be 3.36 eV.

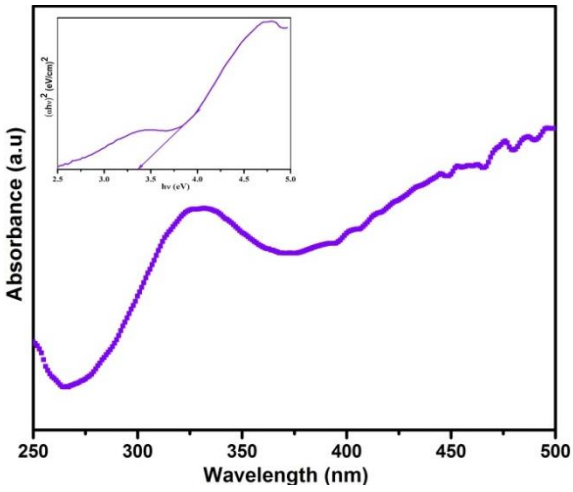

Fig. 3 – UV-visible absorption spectrum and Tauc's plot of SnO_2 nanoparticles

3.4 Humidity Sensing Properties

Relative humidity (RH) is measured by the two-temperature method similar to that reported previously [9]. Nanoparticles are transformed into pellets under a hydraulic press with an applied pressure of 5 tons at RT. The pellet is used as a sensing element. A Chromel/Alumel sensing wire is inserted into the pellet using a silver paste. The humidity sensor system consists of a two-necked round-bottom flask with a capacity of 500 ml. A thermometer is inserted into one neck, and the sensing element, along with another thermometer, is inserted into the other neck. The flask is partially filled with water and kept in an ice-filled glass container. The amount of ice and water is adjusted so as to maintain the water temperature in the flask at the required temperature (T_1). The temperature of the sensing element (T_2), located at a height of 6 cm from the surface of water inside the flask, is monitored using a thermometer at the same level. From the ratio of water vapor pressures at the water temperature (T_1) and the sample (sensing element) temperature (T_2), we can calculate the humidity inside the chamber. A temperature variation of about 5 °C is observed during the experiment. The values of saturated water vapor pressures at the water temperature $E_w(T_1)$ and the sample temperature $E_w(T_2)$ are used to calculate % RH from the equation

$$\% \text{ RH} = \frac{E_w(T_1)}{E_w(T_2)} \times 100.$$

The % RH values are varied by changing the temperature of the water inside the flask with ice and water mixture from RT to 0 °C. The resistance values at different % RH values are measured using a LCR digital meter after the system shows a stable reading within 8-10 min.

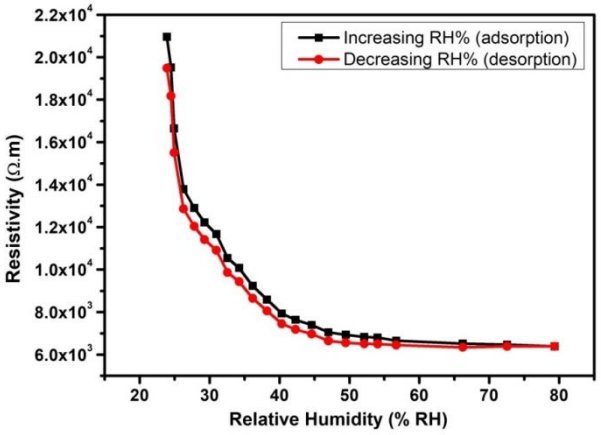

Fig. 4 – Variation of resistivity with RH for a SnO_2-based humidity sensor at RT during adsorption and desorption processes

The humidity sensing properties of the fabricated sensor are measured by exposing the sensor to various relative humidity levels. The variation of resistivity (calculated from the measured resistance values) as a function of RH at RT is shown in Fig. 4. A sharp decrease in the resistivity value is observed till 26 % RH, and then the resistivity gradually decreases in the range 26-56 % RH before attaining saturation in the region 56-80 % RH. Generally, electrons are trapped by surface defects such as oxygen vacancies. When the surface of metal oxides is exposed to humidity, the surface will be covered with hydroxyl groups and hydrogen bonds are formed, providing further adsorption of water molecules [10]. When water molecules are adsorbed by defect sites, electrons trapped in defect sites are released. The observed variation of resistivity may be due to electrons released from water molecules adsorbed on the surface of SnO_2 [11, 12]. The mechanism involved in the humidity sensor is based on absorption and desorption processes that occur between the surface of nanoparticles and humidity. At lower humidity levels, free electrons are trapped as oxygen from the environment is adsorbed by the sensor surface, and thus adsorbed oxygen ions are formed according to the following equation:

$$O_2 + e^- \rightarrow O_{2^-}.$$

When % RH increases, water molecules react with the surface of the sensor via a chemisorption process. During this process, free electrons are released due to the reaction of water molecules with adsorbed oxygen ions:

$$2H_2O + O_{2^-} \rightarrow 2H_2O_2 + e^-.$$

The released free electrons increase the electrical conductivity of the sensor. With further increase in % RH, hydrogen bonds are formed with the primary chemisorbed water layers as water molecules are continuously adsorbed on the sensor surface. Now water molecules adsorbed on the surface of SnO_2 dissociate into H_3O^+ and hydroxyl groups. Then, the metal cation adsorbs hydroxyl groups, which provides mobile protons due to its high electron density and strong electrostatic field. According to the Grotthuss chain reaction, dissociated protons can easily tunnel between adjacent water molecules under an applied electric field [3]. The above process can be expressed as follows:

$$2H_2O \rightarrow H_3O^+ + OH^-,$$

$$H_3O^+ \rightarrow H_2O + H^+.$$

These protons increase the concentration of carriers due to their free movement, and the conductivity is due to the movement of protons from an H_3O^+ ion to an adjacent water molecule and so on. Thus, the observed decrease in the resistivity values with increasing RH can be ascribed to the proton conductivity on the surface of SnO_2 [13, 14]. The fabricated humidity sensor is found to have good sensitivity up to 56 % RH. The observed result is comparable with the previously reported results for SnO_2 nanoparticles prepared by microwave method [11], $ZnSnO_3$ nanoparticles synthesized by chemical precipitation method [15], Fe-doped SnO_2 nanoparticles prepared by co-precipitation method [16], NiO-SnO_2 nanofibers synthesized by electrospinning method [12], and nanocrystalline SnO_2 powders obtained by mechanochemical method [17]. Measurements are also performed by decreasing the % RH from the maximum to study hysteresis behavior which is an important characteristic of a humidity sensor. The adsorption (solid squares) and desorption (solid circles)

curves (Fig. 4) are found to be very close at higher % RH, whereas a small deviation (4-7 %) is observed at lower % RH. The observed hysteresis indicates good reliability of the SnO_2-based humidity sensor. The sensitivity factor is calculated from the formula

$$S(\%) = \frac{|R_0 - R_x|}{R_0},$$

where R_0 is the resistivity value at the lowest RH (24 %) and R_x is the resistivity at any higher RH value. The sensitivity of the SnO_2-based humidity sensor with increasing % RH is shown in Fig. 5.

It is observed that the sensor shows good sensitivity behavior between 24 and 56 % RH, and the highest sensitivity of 70 % is achieved at 80 % RH. The sensitivity of the fabricated SnO_2 sensor is compared with previously reported SnO_2-based sensors and the comparison is given in Table 1.

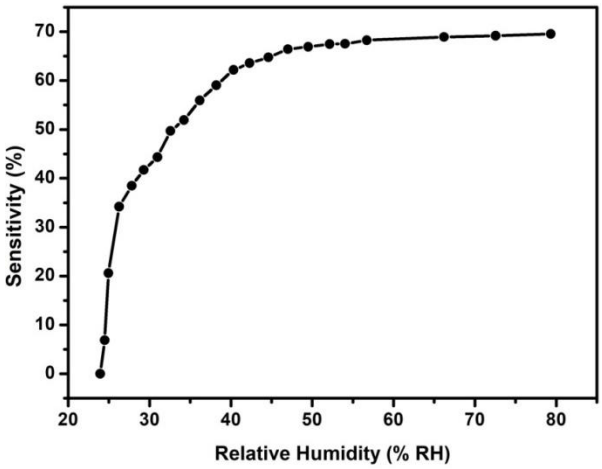

Fig. 5 – Variation of sensitivity of the SnO_2-based sensor with RH at RT

Table 1 – Comparison of humidity sensing performance of the fabricated SnO_2 humidity sensor with previously reported SnO_2-based sensors

Sensing Material	Synthesis Method	Sensor Type	Measurement Range (% RH)	Sensitivity (%)	Reference
SnO_2 nanoparticles	Microwave irradiation	Resistive	5-95	100	Ref [18]
SnO_2 nanostructured films	Nanosphere Lithography	Resistive	11-96	100	Ref [19]
Fe:SnO_2 nanoparticles	Chemical Precipitation	Resistive	0-100	80	Ref [16]
NiO-SnO_2 nanofibers	Electrospinning	Resistive	0-100	82	Ref [12]
SnO_2 thin films	Spin-Spray Process	Resistive	5-95	97	Ref [20]
SnO_2 nanoparticles	Hydrothermal	Resistive	26-80	70	Present work

4. CONCLUSIONS

Synthesis of SnO_2 nanoparticles by employing a surfactant-free hydrothermal approach has been demonstrated in the present work. SnO_2 nanoparticles having a tetragonal rutile structure with high crystalline quality were confirmed by structural analysis using XRD. The SEM micrograph revealed agglomerated nanoparticles having different sizes without any specific structure. The fabricated SnO_2-based humidity sensor exhibited a good response to relative humidity, and the humidity sensing mechanism was explained based on the proton transfer conductivity model. The observed results indicate that by adding suitable dopants to form SnO_2-based nanocomposites, humidity sensing properties can be enhanced.

ACKNOWLEDGEMENTS

This work was financially supported by UGC-DAE-Consortium for Scientific Research (Project Sanction No. CSR-KN/CRS-107/2018-19/1046).

REFERENCES

1. M.S. Chavali, M.P. Nikolova, *SN Appl. Sci.* **1**, s42452 (2019).
2. S.M. Ingole, Y.H. Navale, A.S. Salunkh, M.A. Chougule, G.D. Khuspe, V.B. Patil, *J. Nano- Electron. Phys.* **12** No 2, 02024 (2020).
3. H. Ma, H. Fang, W. Wu, C. Zheng, L. Wu, H. Wang, *RSC Adv.* **10**, 25464 (2020).
4. T. Yang, M. Zhu, K. Gu, C. Zhai, Q. Zhao, X. Yang, M. Zhang, *New J. Chem.* **42**, 13612 (2018).
5. Y. Zhong, W. Li, X. Zhao, X. Jiang, S. Lin, Z. Zhen, W. Chen, D. Xie, H. Zhu, *ACS Appl. Mater. Interfaces* **11** No 14, 13441 (2019).
6. V.K. Tomer, S. Duhan, *Sensor. Actuat. B: Chem.* **223**, 750 (2016).
7. M. Radovic, G. Dubourg, Z. Dohcevic-Mitrovic, B. Stojadinovic, J. Vukmirovic, N. Samardzic, M. Bokorov, *J. Phys. D: Appl. Phys.* **52** No 38, 385305 (2019).
8. V. Kumar, Bhawna, S.K. Yadav, A. Gupta, B. Dwivedi, A. Kumar, P. Singh, K. Deori, *Chem. Sel.* **4** No 13, 3722 (2019).
9. M.V. Kulkarni, A.K. Viswanath, P.K. Khanna, *J. Appl. Polym. Sci.* **99** No 3, 812 (2006).
10. P.A. Thiel, T.E. Madey, *Surface Sci. Rep.* **7** No 6-8, 211 (1987).
11. M. Parthibavarman, V. Hariharan, C. Sekar, *Mater. Sci. Eng. C* **31** No 5, 840 (2011).
12. P. Pascariu, A. Airinei, N. Olaru, I. Petrila, L. Sacarescu, F. Tudorache, *Sensor. Actuat. B Chem.* **222**, 1024 (2016).
13. H. Farahani, R. Wagiran, M.N. Hamidon, *Sensors* **14**, 7881 (2014).
14. M. Sabarilakshmi, K. Janaki, *J. Mater. Sci.: Mater. Electron.* **28**, 5329 (2017).
15. R. Singh, A.K. Yadav, C. Gautam, *J. Sen. Tech.* **1** No 1, 116 (2011).
16. D. Toloman, A. Popa, M. Stan, C. Socaci, A.R. Biris, G. Katona, F. Tudorache, I. Petrila, F. Iacomi., *Appl. Surf. Sci.* **402**, 410 (2017).
17. B.C. Yadav, R. Singh, S. Singh, *J. Exp. NanoSci.* **8** No 5, 670 (2013).

18. S.L. Ko, S. Park, C.W. Kim, D. Lee, M.S. Choi, C. Lee, C. Jin, *Appl. Phys.* A **121**, 715 (2015).
19. W. Li, J. Liu, C. Ding, G. Bai, J. Xu, Q. Ren, J. Li, *Sensors* **17** No 10, 2392 (2017).
20. H.E. Lin, Y. Katayanagi, T. Kishi, T. Yano, N. Matsushita, *RSC Adv.* **8**, 30310 (2018).

Підвищена чутливість до вологості гідротермально синтезованих наночастинок оксиду олова

T. Preethi[1], K. Senthil[1], S. Ashokan[1], R. Balakrishnaraja[2], B. Sundaravel[3], P. Saravanan[4]

[1] *Advanced Materials Research Laboratory, Department of Physics, Bannari Amman Institute of Technology, Sathyamangalam 638401, Tamil Nadu, India*
[2] *Department of Food Technology, Bannari Amman Institute of Technology, Sathyamangalam 638401, Tamil Nadu, India*
[3] *Materials Science Group, Indira Gandhi Centre for Atomic Research, HBNI, Kalpakkam 603102, Tamil Nadu, India*
[4] *Defense Metallurgical Research Laboratory (DMRL), Kanchanbagh, Hyderabad 500058, India*

Метал-оксидні напівпровідникові наноматеріали широко використовуються для застосування в сонячних елементах, акумуляторах, газових датчиках, оптоелектроніці, фотокаталізі та генерації водню. Датчики вологості на основі метал-оксидних напівпровідників показали значний внесок у галузі моніторингу навколишнього середовища, харчових технологій та біотехнологій. Серед різноманітних метал-оксидних напівпровідників наночастинки оксиду олова (SnO_2) викликають більший інтерес завдяки їх високій хімічній стабільності, високій прозорості та низькому електричному поверхневому опору. У роботі наночастинки SnO_2 були синтезовані за допомогою простого гідротермального процесу без використання будь-яких поверхнево-активних речовин. Синтезовані наночастинки досліджували за допомогою XRD, SEM, EDAX, UV-visible та вимірювань вологості. Дослідження структурних властивостей зразків з використанням аналізу XRD свідчать про те, що синтезовані наночастинки SnO_2 мають чисту кристалічну фазу з тетрагональною кристалічною структурою просторової групи P42/mnm. Морфологія поверхні, проаналізована за допомогою мікрофотографії SEM, показала агломеровані наночастинки без будь-якої конкретної структури. Оптична характеризація за допомогою UV-visible спектроскопії виявила, що синтезовані наночастинки мають сильне поглинання в UV області. Чутливість до вологості, проаналізована на основі зміни питомого електричного опору з відносною вологістю (% RH), показала гарну гістерезисну поведінку, а спостережувані зміни електричної провідності пояснюються на основі механізму протонної провідності на поверхні.

Ключові слова: Оксиди металів, Наночастинки SnO_2, Гідротермальний метод, Оптичні властивості, Датчик вологості.